

Bloch-Zener oscillations of strongly correlated electrons

Stefano Longhi

*Dipartimento di Fisica, Politecnico di Milano and Istituto di Fotonica e Nanotecnologie del Consiglio Nazionale delle Ricerche,
Piazza L. da Vinci 32, I-20133 Milano, Italy*

(Received 19 June 2012; published 23 August 2012)

It is well known that an electron in a single-band tight-binding lattice coherently driven by an external dc electric field undergoes Bloch oscillations. In the framework of the extended Hubbard model, here it is shown theoretically that two strongly interacting electrons with on-site and nearest-neighbor site repulsion undergo a sequence of Bloch oscillations and Zener tunneling, the so-called Bloch-Zener oscillations (BZO), among different narrow bands formed by bound particle states. Such a kind of BZO arise because of nearest-neighbor site particle interaction and are thus rather distinct than BZO observed for a single electron in biperiodic lattices supporting two single-particle minibands.

DOI: [10.1103/PhysRevB.86.075144](https://doi.org/10.1103/PhysRevB.86.075144)

PACS number(s): 71.10.Fd, 67.85.-d, 73.21.Cd

I. INTRODUCTION

Bloch oscillations (BOs) and Zener tunneling (ZT) are fundamental coherent transport phenomena that occur when electrons in a periodic potential are accelerated by an external dc electric field.^{1–3} While in natural crystals electronic BOs can not be observed owing to dephasing effects, BOs and ZT have been impressively demonstrated in a number of experiments after the advent of semiconductor superlattices.⁴ Quantum and classical analogues of BOs and ZT have been also proposed and observed in a wide variety of different physical systems, including ultracold atoms⁵ and Bose-Einstein condensates,⁶ optical waveguide arrays,⁷ photonic⁸ and acoustic⁹ superlattices. In a tight-binding (single band) lattice model, BOs basically arise because the energy spectrum changes from continuous (a band structure with delocalized Bloch eigenstates) in absence of the external field, to a discrete ladder energy spectrum and localized eigenfunctions (the Wannier-Stark spectrum) when the external field is applied. For biperiodic systems sustaining two bands energetically separated from higher bands (miniband structure), a characteristic sequence of BOs and ZT between the two minibands, the so-called Bloch-Zener oscillations (BZO), have been predicted^{10–12} and recently observed for optical¹³ and matter waves.¹⁴ In the driven binary superlattice, the single-particle energy spectrum is composed by two interleaved Wannier-Stark ladders and BZO are thus generally aperiodic.

The onset of BOs may be affected rather dramatically by particle interactions, lattice disorder, inhomogeneities, and particle statistics (see, for instance, Refs. 15–23 and references therein). In particular, several recent works have investigated theoretically BOs in the framework of Hubbard or Bose-Hubbard models beyond mean-field models.^{17–22} As correlation is generally responsible for decoherence of BOs,^{17,18} interesting novel phenomena have been predicted for BOs of *few* interacting particles in the strong interaction regime,^{19–21} such as the frequency doubling of BOs of two correlated particles^{19,20} and, more generally, fractional BOs for *N*-bound particle states.²¹ Such a behavior basically stems from the fact that two strongly interacting particles initially occupying the same site form a bound pair,²⁴ undergoing correlated tunneling on the lattice.²⁵

In this work, the coherent dynamics of two strongly interacting electrons with opposite spins in driven one-dimensional tight-binding lattices with on-site and nearest-neighbor site repulsion is theoretically investigated in the framework of the extended Hubbard model.²⁶ The main result of the analysis is that, as the tight-binding lattice supports a single band and a single electron forced by an external dc field undergoes ordinary BOs, two correlated electrons undergo BZO involving different bands of interaction-induced bound particle states. Such a kind of BZO are a clear signature of the near-neighbor site repulsion and are thus rather distinct than BZO observed for a single electron in biperiodic lattices supporting two single-particle minibands.

II. TWO-ELECTRON DYNAMICS IN THE EXTENDED HUBBARD MODEL

The starting point of the analysis is provided by the driven one-dimensional extended Hubbard model (EHM), that describes the hopping dynamics of correlated electrons on a one-dimensional tight-binding lattice driven by an external dc electric field. The EHM is defined by the Hamiltonian²⁶

$$\hat{H} = -J \sum_{l,\sigma=\uparrow,\downarrow} \hat{a}_{l,\sigma}^\dagger (\hat{a}_{l-1,\sigma} + \hat{a}_{l+1,\sigma}) + U \sum_l \hat{n}_{l,\uparrow} \hat{n}_{l,\downarrow} + V \sum_l \hat{n}_l \hat{n}_{l+1} + eEd \sum_l l \hat{n}_l. \quad (1)$$

In Eq. (1), $\hat{a}_{l,\sigma}^\dagger$ are $\hat{a}_{l,\sigma}$ are the fermionic creation and annihilation operators of electrons with spin $\sigma = \uparrow, \downarrow$ at lattice sites $l = 0, \pm 1, \pm 2, \dots$, J is the single-particle hopping rate between adjacent sites, $U > 0$ and $V > 0$ define the on-site and nearest-neighbor Coulomb repulsion, respectively, d is the lattice period, E is the external dc electric field, $\hat{n}_{l,\sigma} = \hat{a}_{l,\sigma}^\dagger \hat{a}_{l,\sigma}$, and $\hat{n}_l = \hat{n}_{l,\uparrow} + \hat{n}_{l,\downarrow}$ is the particle number operator. The EHM is a prototype model in condensed matter theory, which exhibits a rich phase diagram.²⁶ As compared to the standard Hubbard model [which is obtained by letting $V = 0$ in Eq. (1)], the EHM accounts for the nonlocal interaction arising from Coulomb repulsion of electrons in adjacent sites due to nonperfect screening of electronic charges. Additional terms, accounting for long-range Coulomb repulsion (for example, between next-nearest neighbors), might be included in the

Hamiltonian (1). It should be noted that Eq. (1) may also describe fermionic ultracold atoms or molecules with magnetic or electric dipole-dipole interactions in optical lattices. In this case, the sign of U and V can be reversed, and the ratio V/U can be tuned by modifying the trap geometry of the condensate, additional external dc electric fields, combinations with fast rotating external fields, etc. (see, for instance, Ref. 27 and references therein). In the present work, we will assume for the sake of definiteness $U, V > 0$, and we will mainly focus our analysis by considering only the nearest-neighbor Coulomb repulsion. The Hubbard Hamiltonian (1) conserves the total number of electrons, as well as the total number of electrons N_\downarrow, N_\uparrow with spin down and up. As in Refs. 19 and 20, we consider the coherent motion of two correlated electrons with opposite spins driven by the external dc field, i.e., $N_\downarrow = N_\uparrow = 1$, and we wish to highlight the impact of the nearest-neighbor repulsion V on the BO dynamics. To this aim, let us indicate by $c_{n,m}(t)$ the amplitude probability to find the electron with spin \uparrow at lattice site n and the electron with spin \downarrow at lattice site m , i.e., let us expand the state vector $|\psi(t)\rangle$ of the system in Fock space as

$$|\psi(t)\rangle = \sum_{n,m} c_{n,m}(t) \hat{a}_{n,\uparrow}^\dagger \hat{a}_{m,\downarrow}^\dagger |0\rangle. \quad (2)$$

The evolution equations for the amplitude probabilities $c_{n,m}$, as obtained from the Schrödinger equation $i\partial_t |\psi\rangle = \hat{H} |\psi\rangle$ with $\hbar = 1$, read explicitly

$$i \frac{dc_{n,m}}{dt} = -J(c_{n+1,m} + c_{n-1,m} + c_{n,m-1} + c_{n,m+1}) + [U\delta_{n,m} + V\delta_{n,m+1} + V\delta_{n,m-1} + F(n+m)]c_{n,m}, \quad (3)$$

where we have set $F = eEd$. In the strong interaction and low-field regimes, corresponding to $J, F \ll U, V$, at leading order the dynamics in Fock space for the amplitudes $c_{n,m}$ with $m = n, n \pm 1$ decouples from the other states.²⁸ Therefore, if we assume that the two electrons are initially placed at the same lattice site or in nearest sites, i.e., if we assume $c_{n,m}(0) = 0$ for $m \neq n, n \pm 1$ as an initial condition, Eq. (3) reduce to the following set of coupled equations:

$$\begin{aligned} i \frac{dA_n}{dt} &= -J(B_n + B_{n-1} + C_n + C_{n-1}) + UA_n + 2nFA_n, \\ i \frac{dB_n}{dt} &= -J(A_n + A_{n+1}) + VB_n + (2n+1)FB_n, \\ i \frac{dC_n}{dt} &= -J(A_n + A_{n+1}) + VC_n + (2n+1)FC_n, \end{aligned} \quad (4)$$

where we have set

$$A_n = c_{n,n}, \quad B_n = c_{n,n+1}, \quad C_n = c_{n+1,n}. \quad (5)$$

III. BLOCH-ZENER OSCILLATIONS OF STRONGLY CORRELATED ELECTRONS

The effect of the on-site Coulomb interaction on BOs for two strongly correlated electrons, corresponding to the limiting case $V = 0$, has been studied in Refs. 19 and 20. In those works, it was shown that two electrons initially occupying the same site and driven by the external dc field

undergo correlated BOs with a frequency twice the BOs frequency of the single-particle (noninteracting) problem. The frequency doubling follows from the circumstance that two strongly-interacting electrons initially occupying the same site form a bound pair with an effective $2e$ charge and tunnel together on the lattice.^{19,20}

Here, we show that if nearest-neighbor repulsion is included in the analysis, two strongly correlated electrons undergo BZO, rather than simple BOs. Let us first observe that in the absence of the dc field, i.e., for $F = 0$, the energy spectrum of the two-electron state comprises three Bloch bands, one of which being collapsed and corresponding to localized states (see Appendix and also Ref. 29). As the external field is switched on, the energy spectrum ϵ of the two correlated electrons becomes discrete and turns out to be composed by *three* interleaved Wannier-Stark ladders:

$$\epsilon_l^{(j)} = U + 2F(l - \mu_j) \quad (6)$$

($l = 0, \pm 1, \pm 2, \pm 3, \dots, j = 1, 2, 3$), where μ_j are three characteristic functions of $[(U - V)/J, F/J]$ corresponding to the Floquet exponents of a linear periodic system. The proof thereof as well as the determination of the Floquet exponents $\mu_j[(U - V)/J, F/J]$ are detailed in Appendix. Therefore an initial wave packet undergoes a quasiperiodic dynamics, characterized by different temporal scales defined by the energy level spacings of the discrete spectrum [see Eq. (6)]. For special values of the Floquet exponents, the energy levels can be arranged to be equally spaced. In this case, the dynamics turns out to be periodic. More generally, the dynamics turns out to be periodic whenever μ_1, μ_2 , and μ_3 are rational numbers. Similarly to the BZO of single electrons in binary superlattices,^{10,11} the onset of BZO can be explained as a sequence of BOs and ZT among the Bloch bands of bound particle states induced by the external electric field.

It should be noted that, for an initial condition satisfying the constraint $c_{n,n+1}(0) = c_{n+1,n}(0)$ (for example, whenever the two electrons are initially placed on the same lattice site and thus $c_{n,n+1}(0) = c_{n+1,n}(0) = 0$), only two Wannier-Stark ladders are excited, and a two-band dynamics is attained, similar to the BZO of a single electron in a binary superlattice. In fact, if $B_n(0) = C_n(0)$, the solution to Eq. (4) satisfies the constraint $C_n(t) = B_n(t)$ at any time $t \geq 0$. After setting

$$A_n(t) = f_{2n}(t) \exp[-i(U + V)t/2], \quad (7)$$

$$B_n(t) = \frac{1}{\sqrt{2}} f_{2n+1}(t) \exp[-i(U + V)t/2], \quad (8)$$

the dynamics of the amplitudes $f_n(t)$, as obtained from Eq. (4) using Eqs. (7) and (8), reads

$$i \frac{df_n}{dt} = -\sqrt{2}J(f_{n+1} + f_{n-1}) + Fn f_n + (-1)^n \sigma f_n, \quad (9)$$

where we have set $\sigma \equiv (U - V)/2$. In their present form, Eq. (9) are formally analogous to the tight-binding model describing the hopping dynamics of a single electron in a binary superlattice driven by the external dc force $F = edE$,¹⁰ the energy difference 2σ between adjacent lattice sites being determined by the unbalance $(U - V)$ of on-site and nearest-neighbor site repulsion in the original problem. Hence for the initial conditions $c_{n,m}(0) = A_n(0)\delta_{n,m}$, the two strongly

interacting electrons undergo BZO involving solely two bands. In particular, for $U = V$ one obtains the ordinary BOs of the single-particle problem. This means that, if $U = V$ and the two electrons are initially placed on the same lattice site, frequency doubling of BOs predicted in the framework of the ordinary Hubbard model²⁰ disappears, and the two electrons undergo correlated BOs with the same frequency as for the single-particle problem.

We have checked the predictions of our analysis, based on the truncated Eq. (4) and Floquet analysis provided in Appendix, by direct numerical simulations of the EHM [see Eq. (1)] for two strongly correlated electrons. The results are obtained by numerical simulations of Eq. (3) using an accurate fourth-order variable-step Runge-Kutta method in a truncated lattice comprising 31 sites ($-15 \leq n, m \leq 15$). In a first set of simulations, we typically fixed the values of on-site and nearest-neighbor site repulsion to $U/J = 20$ and $V/J = 19.2$, respectively, and vary the ratio F/J to explore different dynamical regimes. Note that, since $V \neq U$, BZOs—rather than simple BOs—are expected to be observed according to the previous analysis. The behavior of the Floquet exponents μ_1 , μ_2 , and μ_3 versus F/J , numerically computed using the procedure outlined in Appendix, is depicted in Fig. 1. For an initial condition corresponding to the two electrons placed

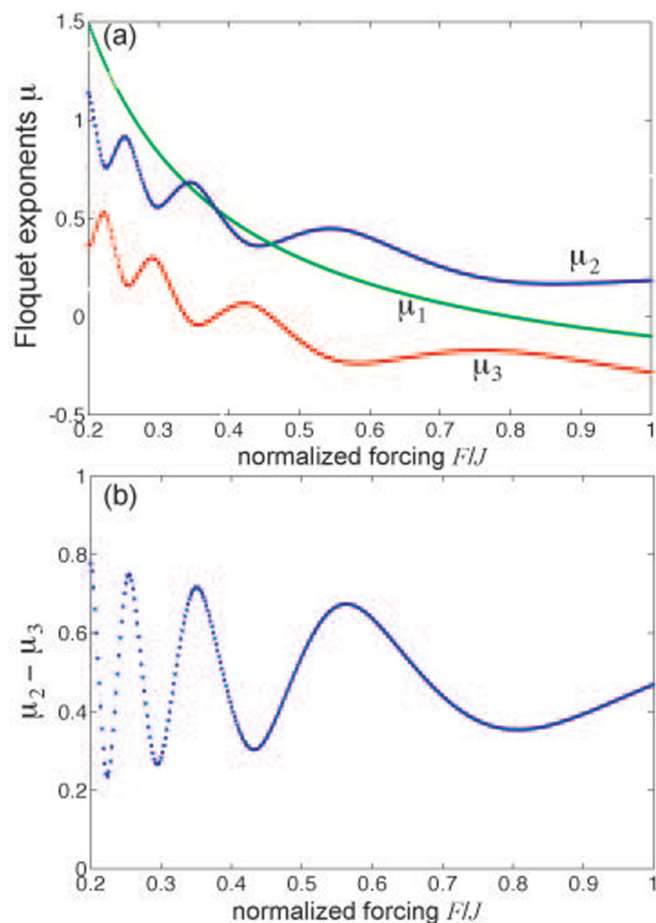


FIG. 1. (Color online) (a) Behavior of the Floquet exponents μ_j ($j = 1, 2, 3$), defining the relative positions of the Wannier-Stark ladders [see Eq. (6) in the text], vs F/J for $(U - V)/J = 0.2$. The plot in (b) shows the behavior of the difference $\mu_2 - \mu_3$.

on the same lattice site, i.e., for $c_{n,m}(0) = A_n(0)\delta_{n,m}$ with some distribution $A_n(0)$, only the two WS ladders $\epsilon_l^{(2)}$ and $\epsilon_l^{(3)}$ are excited, and the dynamics turns out to be generally quasiperiodic with the two characteristic time scales:^{10,13}

$$T_1 = \frac{\pi}{F}, \quad T_2 = \frac{\pi}{F|\mu_2 - \mu_3|}. \quad (10)$$

If the ratio $T_1/T_2 = |\mu_2 - \mu_3| = N/M$ is a rational number (with N and M irreducible integer numbers), then the

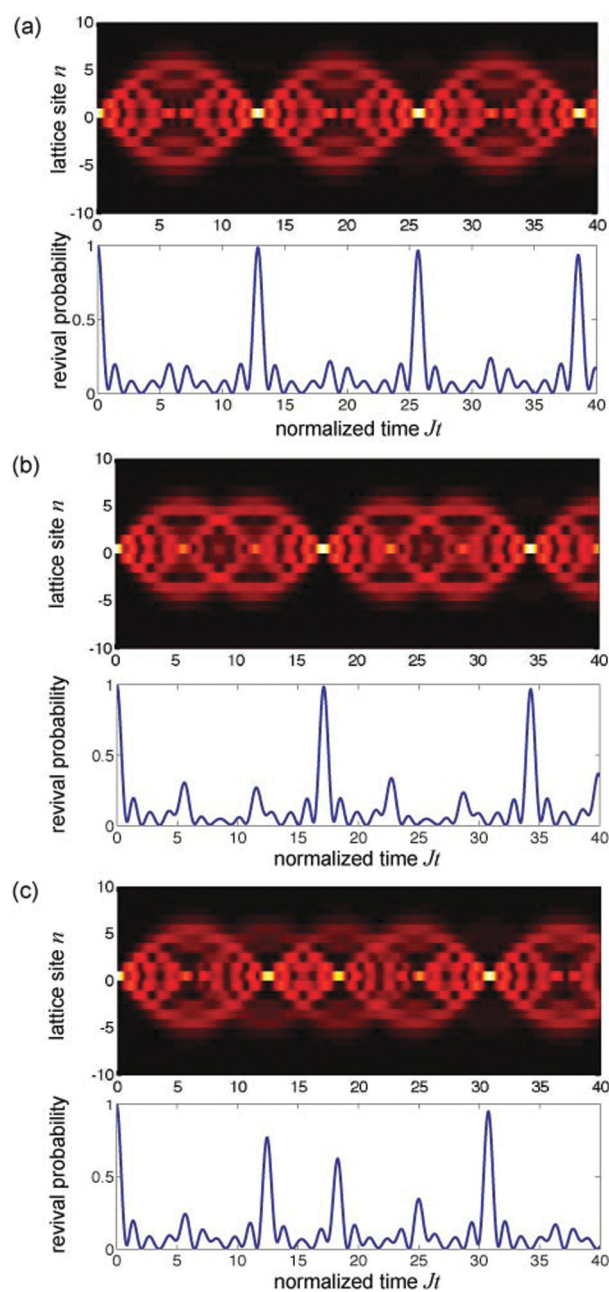


FIG. 2. (Color online) Numerically computed evolution of the square root of the joint probability $P^{(2)}(n) = |c_{n,n}(t)|^2$ (upper plots) and of the revival probability $P_r(t)$ (lower plots) for $U/J = 20$, $V/J = 19.2$, and for a few values of the forcing: (a) $F/J = 0.49$, (b) $F/J = 0.55$, and (c) $F/J = 0.5167$. The initial condition is $c_{n,m}(0) = \delta_{n,0}\delta_{m,0}$, corresponding to the two electrons initially placed at the same lattice site $n = 0$.

dynamics is periodic with a period

$$T = NT_2 = MT_1 = \frac{M\pi}{F}. \quad (11)$$

As an example, Figs. 2(a)–2(c) show the numerically computed temporal evolution of the square root of the joint probability $P_n^{(2)}(t) = |c_{n,n}(t)|^2$ to find both electrons at the same lattice site n for the initial condition $A_n(0) = \delta_{n,0}$ (corresponding to the two electrons initially placed at the same lattice site $n = 0$) and for three values of F/J , corresponding to $\mu_2 - \mu_3 \simeq 1/2$, $\mu_2 - \mu_3 \simeq 2/3$, and $\mu_2 - \mu_3 \simeq 3/5$, respectively. The evolution of the revival probability

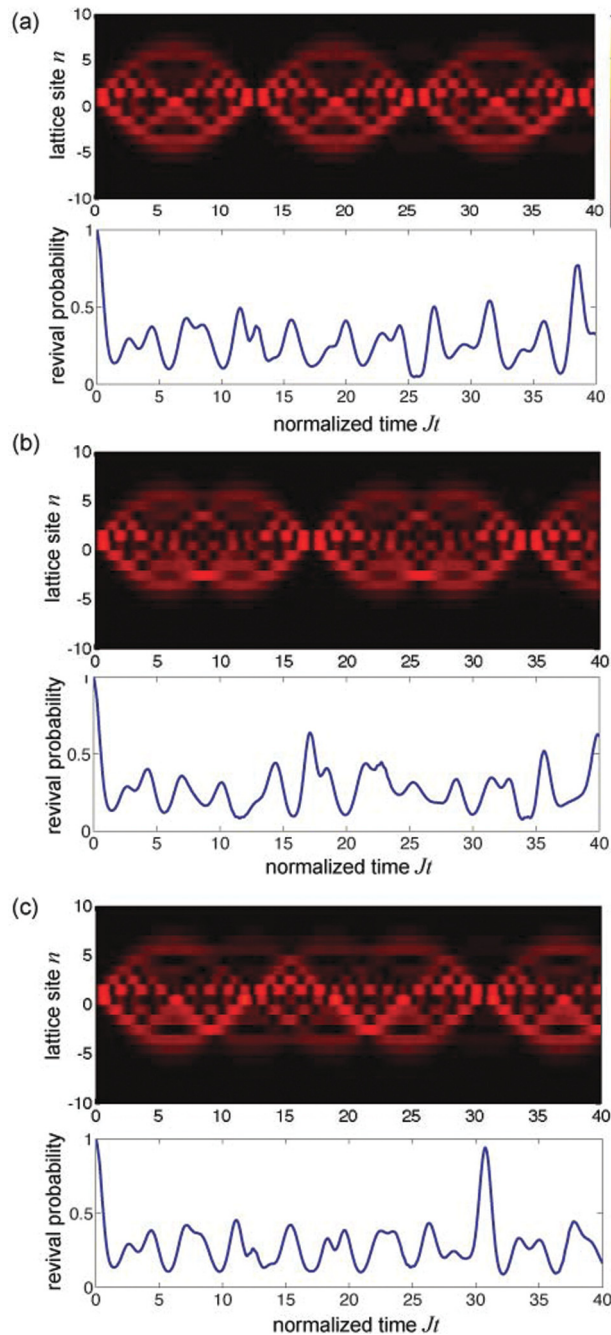


FIG. 3. (Color online) Same as Fig. 2, but for the initial condition $c_{n,m}(0) = \delta_{n,0}\delta_{m,1}$.

$P_r(t) = |\langle \psi(t) | \psi(0) \rangle|^2$ is also depicted. For such an initial condition (single-site excitation), BZO are visualized as a periodic or quasi-periodic breathing dynamics of the electronic wave packet.^{10,13} In Figs. 2(a)–2(c), the breathing dynamics of both revival and joint probabilities is appreciably periodic with periods $T = 2\pi/F$, $T = 3\pi/F$, and $T = 5\pi/F$, respectively. Such results are in excellent agreement with the theoretical prediction [see Eq. (11) with $M = 2, 3$, and 5 , respectively].

If the two electrons are initially placed at the nearest lattice sites, the three WS ladders are simultaneously excited and the dynamics generally involves three distinct time scales. As an example, in Fig. 3, we show the evolution of the revival probability $P_r(t)$ and of the square root of the joint probability $P_n^{(2)}(t)$ for the same parameter values as in Fig. 2, except for the different initial condition $c_{n,m}(0) = \delta_{n,0}\delta_{m,1}$. Note that the periodicity of the revival probability, found in Fig. 2, is now broken, in spite, the joint probability remains periodic. This is due to the fact that the solution to $c_{n,m}(t)$ is given by the superposition of the two WS ladders $\epsilon_l^{(2,3)}$ solely for $(n,m) \neq (0, \pm 1)$, whereas the amplitudes $c_{0,\pm 1}(t)$ show an additional contribution arising from the excitation of the bound state with energy $\epsilon_l^{(1)}$ (see Appendix for details). Such a circumstance explains why the evolution of the joint probability in Fig. 3 remains periodic, whereas the revival probability is not periodic.

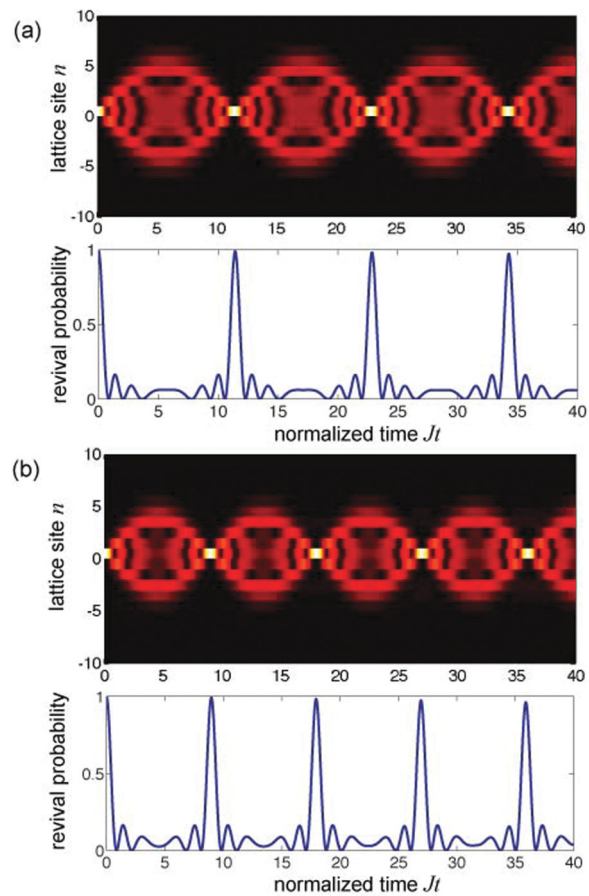


FIG. 4. (Color online) Same as Fig. 2, but for $V/J = U/J = 20$. In (a) $F/J = 0.55$, whereas in (b) $F/J = 0.7$. The initial condition is $c_{n,m}(0) = \delta_{n,0}\delta_{m,0}$. Note that the BO period is given by $T = 2\pi/F$.

In a second set of simulations, we fixed $V = U$ and checked the disappearance of BO frequency doubling, predicted for two strongly correlated electrons in the framework of the standard Hubbard model, i.e., in the absence of the nearest-neighbor site interaction ($V = 0$).^{19–21} As an example, Fig. 4 shows the evolution of both revival and joint probabilities for $U/J = V/J = 20$ and for two values of the external field, assuming as an initial condition that the two electrons are placed at the same lattice site $n = 0$ (i.e., $c_{n,m} = \delta_{n,0}\delta_{m,0}$). According to the theoretical analysis, in this case simple, BOs—rather than BZO—are observed, with a period $T = 2\pi/F$ equal to the single-particle BO period.

IV. CONCLUSIONS AND DISCUSSION

In this work, the coherent dynamics of two strongly interacting electrons with opposite spins in one-dimensional tight-binding lattices with on-site U and nearest-neighbor site V repulsion driven by a dc electric field has been theoretically investigated in the framework of the extended Hubbard model. The analysis shows that in the strong interaction regime and for $V \neq U$ the two electrons undergo a sequence of Bloch oscillations and Zener tunneling, the so-called Bloch-Zener oscillations, among different bands of bound particle states. For $V = U$, ordinary BOs should be observed with a period equal to the single-particle BO period. This result is rather distinct than the prediction of frequency doubling of BOs for two strongly correlated electrons that one would expect in the framework of the standard Hubbard model.^{20,21}

BZO predicted in this work are a clear signature of nearest-neighbor site particle interaction and are expected to be observable in quantum²⁷ or classical³⁰ simulators of the extended Hubbard model. For example, a photonic simulator of the EHM for two interacting electrons with opposite spin driven by an external dc field can be realized by considering transport of classical light in a square array of coupled optical waveguides with a circularly curved optical axis and with defects along three adjacent diagonals, extending the optical setup suggested in Ref. 30 to simulate correlated BOs in the framework of the standard Hubbard model. In fact, Eq. (3) clearly shows that the dynamics of the two interacting electrons in a one-dimensional lattice is equivalent to the dynamics of a single particle hopping on a two-dimensional square lattice, with energy site impurities U and V on the main ($m = n$) and nearest ($m = n \pm 1$) diagonals of the lattice, respectively.

As a final comment, it is worth briefly commenting on the effects of non-nearest-neighbor (long-range) electron-electron repulsions in the EHM, which have been neglected in Eq. (1). For example, the inclusion of the next-nearest-neighbor repulsion corresponds to add, in the Hamiltonian (1), a term

of the form $W \sum_l \hat{n}_l \hat{n}_{l+2}$, where W measures the strength of the next-nearest-neighbor electron-electron repulsion. In the strong interaction limit, assuming $U, V, W \gg J$, the dynamics in Fock space of the amplitude probabilities $c_{n,m}(t)$ for two electrons with opposite spins [see Eq. (3)] decouples the amplitudes $c_{n,n}$, $c_{n,n\pm 1}$, and $c_{n,n\pm 2}$ from the other ones. Extending the procedure outlined in the Appendix, one then would obtain that the energy spectrum of the Hamiltonian in the truncated Fock space and in the absence of the electric field comprises five bands, corresponding to five bound particle states. As the electric field is switched on, the spectrum becomes discrete and comprises five interleaved Wannier-Stark ladders. Therefore two coherently driven strongly interacting electrons undergo again BZO, involving this time five bands, which are generally aperiodic. Extending the setup proposed in Ref. 30, the EHM with nearest and next-nearest electron-electron repulsion can be simulated in a square photonic lattice with defects on five (rather than three) lattice diagonals.

ACKNOWLEDGMENTS

The author acknowledges financial support by the Italian MIUR (Grant No. PRIN-2008-YCAAK).

APPENDIX: DETERMINATION OF THE WANNIER-STARK ENERGY SPECTRUM

The energy spectrum ϵ of two strongly-correlated electrons is provided by the eigenvalues of the coupled equations (4), i.e., by the eigenvalues of the linear system

$$\begin{aligned} \epsilon A_n &= -J(B_n + B_{n-1} + C_n + C_{n-1}) + U A_n + 2n F A_n, \\ \epsilon B_n &= -J(A_n + A_{n+1}) + V B_n + (2n + 1) F B_n, \\ \epsilon C_n &= -J(A_n + A_{n+1}) + V C_n + (2n + 1) F C_n. \end{aligned} \quad (\text{A1})$$

To determine the eigenvalues ϵ , let us introduce the three Bloch functions

$$\begin{aligned} A(q) &= \sum_{n=-\infty}^{\infty} A_n \exp(iqn), \\ B(q) &= \sum_{n=-\infty}^{\infty} B_n \exp(iqn), \\ C(q) &= \sum_{n=-\infty}^{\infty} C_n \exp(iqn), \end{aligned} \quad (\text{A2})$$

which are obviously periodic functions of q with period 2π . From Eqs. (A1) and (A2), one can readily obtain the following coupled equations for the Bloch functions $A(q)$, $B(q)$, and $C(q)$:

$$\frac{d}{dq} \begin{pmatrix} A \\ B \\ C \end{pmatrix} = \frac{i}{2F} \begin{pmatrix} \epsilon - U & J[1 + \exp(iq)] & J[1 + \exp(iq)] \\ J[1 + \exp(-iq)] & \epsilon - V - F & 0 \\ J[1 + \exp(-iq)] & 0 & \epsilon - V - F \end{pmatrix} \begin{pmatrix} A \\ B \\ C \end{pmatrix}. \quad (\text{A3})$$

After setting

$$\begin{pmatrix} A \\ B \\ C \end{pmatrix} = \begin{pmatrix} a \\ b \\ c \end{pmatrix} \exp[i(\epsilon - U)q/2F], \quad (\text{A4})$$

the vector $\mathbf{v}(q) \equiv (a, b, c)^T$ satisfies the following linear system with periodic coefficients:

$$\frac{d\mathbf{v}}{dq} = i\mathcal{M}(q)\mathbf{v}, \quad (\text{A5})$$

where the 2π -periodic matrix $\mathcal{M}(q)$ is given by

$$\mathcal{M}(q) = \frac{J}{2F} \begin{pmatrix} 0 & 1 + \exp(iq) & 1 + \exp(iq) \\ 1 + \exp(-iq) & (U - V - F)/J & 0 \\ 1 + \exp(-iq) & 0 & (U - V - F)/J \end{pmatrix}. \quad (\text{A6})$$

Equation (A5) should be integrated in the interval $(0, 2\pi)$ with the boundary condition

$$\mathbf{v}(2\pi) = \mathbf{v}(0) \exp[-i\pi(\epsilon - U)/F], \quad (\text{A7})$$

which follows from the 2π periodicity of the Bloch functions $A(q)$, $B(q)$, $C(q)$ and from the ansatz (A4). On the other hand, for the Floquet theorem of periodic linear systems, the solution to Eq. (A5) has the form

$$\mathbf{v}(q) = \mathcal{P}(q) \exp(i\mathcal{S}q)\mathbf{v}(0), \quad (\text{A8})$$

where $\mathcal{P}(0) = \mathcal{I}$ is the identity matrix, $\mathcal{P}(q + 2\pi) = \mathcal{P}(q)$, and \mathcal{S} is a 3×3 constant matrix (i.e., independent of q). The eigenvalues μ_1 , μ_2 , and μ_3 of \mathcal{S} are called the Floquet exponents of the linear periodic system (A5). From Eqs. (A7) and (A8) it then follows that

$$\exp[-i\pi(\epsilon - U)/F]\mathbf{v}(0) = \exp(2\pi i\mathcal{S})\mathbf{v}(0), \quad (\text{A9})$$

i.e., $\exp[-i\pi(\epsilon - U)/F]$ is an eigenvalue of the exponential matrix $\exp(2\pi i\mathcal{S})$. Since the eigenvalues of $\exp(2\pi i\mathcal{S})$ are $\exp(2\pi i\mu_j)$ ($j = 1, 2, 3$), where μ_j are the Floquet exponents, one then obtains

$$\epsilon = \epsilon_l^{(j)} = U + 2F(l - \mu_j), \quad (\text{A10})$$

where $l = 0, \pm 1, \pm 2, \pm 3, \dots$ is an arbitrary integer. Note that the Floquet exponents μ_j turn out to be continuous functions of $(U - V)/J$ and F/J [see Eq.(A6)]. They can be numerically determined by standard methods by solving the periodic system (A5) in the interval $(0, 2\pi)$. According to Eq. (A10), the energy spectrum of two strongly correlated electrons is thus purely discrete and given by three interleaved Wannier-Stark ladders. It is worth noticing that, owing to the structure of the matrix $\mathcal{M}(q)$, the linearly independent solutions to the system (A5) correspond to either $b = c, a \neq 0$ or $b = -c, a = 0$. In the latter case, one obtains

$$\frac{dc}{dq} = i \frac{U - V - F}{2F} c, \quad (\text{A11})$$

whereas in the former case one has

$$\frac{d}{dq} \begin{pmatrix} a \\ b \end{pmatrix} = i\mathcal{R}(q) \begin{pmatrix} a \\ b \end{pmatrix}, \quad (\text{A12})$$

where the 2×2 periodic matrix $\mathcal{R}(q)$ is given by

$$\mathcal{R}(q) = \frac{J}{2F} \begin{pmatrix} 0 & 2[1 + \exp(iq)] \\ 1 + \exp(-iq) & (U - V - F)/J \end{pmatrix}. \quad (\text{A13})$$

From Eq. (A11) it follows that one Floquet exponent, say μ_1 , is merely given by

$$\mu_1 = \frac{U - V - F}{2F}, \quad (\text{A14})$$

leading to the Wannier-Stark ladder

$$\epsilon_l^{(1)} = (2l + 1)F + V. \quad (\text{A15})$$

The corresponding Wannier-Stark eigenstates are merely given by $A_n = c_{n,n} = 0$, $B_n = c_{n,n+1} = (1/\sqrt{2})\delta_{n,l}$, $C_n = c_{n+1,n} = -(1/\sqrt{2})\delta_{n,l}$, i.e., they are the entangled bound states $(1/\sqrt{2})(\hat{a}_{l,\uparrow}^\dagger \hat{a}_{l+1,\downarrow}^\dagger - \hat{a}_{l+1,\uparrow}^\dagger \hat{a}_{l,\downarrow}^\dagger)|0\rangle$. The other two Floquet exponents μ_2 and μ_3 are the Floquet exponents associated to the system (A12).

Let us finally notice that, in the absence of the external field, i.e., for $F = 0$, the energy spectrum ϵ is purely continuous and composed by three bands. The dispersion relations $\epsilon_j(q)$ for the three bands ($j = 1, 2, 3$) are readily obtained from Eq. (A3) after setting $F \rightarrow 0$, i.e., they are the roots of the determinantal equation

$$\begin{vmatrix} \epsilon(q) - U & J[1 + \exp(iq)] & J[1 + \exp(iq)] \\ J[1 + \exp(-iq)] & \epsilon(q) - V & 0 \\ J[1 + \exp(-iq)] & 0 & \epsilon(q) - V \end{vmatrix} = 0. \quad (\text{A16})$$

One then obtains

$$\epsilon_1(q) = V, \quad (\text{A17})$$

$$\epsilon_2(q) = \frac{U + V}{2} + \sqrt{\left(\frac{U - V}{2}\right)^2 + 8J^2 \cos^2\left(\frac{q}{2}\right)}, \quad (\text{A18})$$

$$\epsilon_3(q) = \frac{U + V}{2} - \sqrt{\left(\frac{U - V}{2}\right)^2 + 8J^2 \cos^2\left(\frac{q}{2}\right)}. \quad (\text{A19})$$

Note that the first band $\epsilon_1(q)$ is collapsed, and corresponds to a degenerate set of bound states $c_{n,n+1} = -c_{n+1,n} =$

$(1/\sqrt{2})\exp(-iVt)$ and $c_{l,k} = 0$ otherwise. The collapse of the band is a rigorous result in the strong interaction limit $U/J, V/J \rightarrow \infty$ considered in this work, which justifies trun-

cation (4) of the system (3). For finite values $U/J, V/J$, a regular (not collapsed) band is obtained, which corresponds to the energy branch of asymmetric bound states discussed in Ref. 29.

-
- ¹F. Bloch, *Z. Phys.* **52**, 555 (1928); C. Zener, *Proc. R. Soc. London A* **145**, 523 (1934).
- ²J. Callaway, *Quantum Theory of the Solid State* (Academic Press, New York, 1974), pp. 465–478.
- ³M. Glück, A. R. Kolovsky, and H. J. Korsch, *Phys. Rep.* **366**, 103 (2002); A. R. Kolovsky and H. J. Korsch, *Int. J. Mod. Phys.* **18**, 1235 (2004).
- ⁴J. Feldmann, K. Leo, J. Shah, D. A. B. Miller, J. E. Cunningham, T. Meier, G. von Plessen, A. Schulze, P. Thomas, and S. Schmitt-Rink, *Phys. Rev. B* **46**, 7252 (1992); T. Dekorsy, P. Leisching, K. Köhler, and H. Kurz, *ibid.* **50**, 8106 (1994); C. Waschke, H. G. Roskos, R. Schwedler, K. Leo, H. Kurz, and K. Köhler, *Phys. Rev. Lett.* **70**, 3319 (1993); K. Leo, *Semicond. Sci. Technol.* **13**, 249 (1998).
- ⁵M. Ben Dahan, E. Peik, J. Reichel, Y. Castin, and C. Salomon, *Phys. Rev. Lett.* **76**, 4508 (1996); S. R. Wilkinson, C. F. Bharucha, K. W. Madison, Q. Niu, and M. G. Raizen, *ibid.* **76**, 4512 (1996).
- ⁶B. P. Anderson and M. A. Kasevich, *Science* **282**, 1686 (1998); O. Morsch, J. H. Müller, M. Cristiani, D. Ciampini, and E. Arimondo, *Phys. Rev. Lett.* **87**, 140402 (2001); G. Roati, E. de Mirandes, F. Ferlaino, H. Ott, G. Modugno, and M. Inguscio, *ibid.* **92**, 230402 (2004).
- ⁷R. Morandotti, U. Peschel, J. S. Aitchison, H. S. Eisenberg, and Y. Silberberg, *Phys. Rev. Lett.* **83**, 4756 (1999); T. Pertsch, P. Dannberg, W. Elflein, A. Bräuer, and F. Lederer, *ibid.* **83**, 4752 (1999); H. Trompeter, T. Pertsch, F. Lederer, D. Michaelis, U. Streppel, A. Bräuer, and U. Peschel, *ibid.* **96**, 023901 (2006); N. Chiodo, G. Della Valle, R. Osellame, S. Longhi, G. Cerullo, R. Ramponi, P. Laporta, and U. Morgner, *Opt. Lett.* **31**, 1651 (2006); H. Trompeter, W. Krolikowski, D. N. Neshev, A. S. Desyatnikov, A. A. Sukhorukov, Yu. S. Kivshar, T. Pertsch, U. Peschel, and F. Lederer, *Phys. Rev. Lett.* **96**, 053903 (2006).
- ⁸R. Sapienza, P. Costantino, D. Wiersma, M. Ghulinyan, C. J. Oton, and L. Pavesi, *Phys. Rev. Lett.* **91**, 263902 (2003); V. Agarwal, J. A. del Rio, G. Malpuech, M. Zamfirescu, A. Kavokin, D. Coquillat, D. Scalbert, M. Vladimirova, and B. Gil, *ibid.* **92**, 097401 (2004).
- ⁹H. Sanchis-Alepuz, Y. A. Kosevich, and J. Sanchez-Dehesa, *Phys. Rev. Lett.* **98**, 134301 (2007); Z. He, S. Peng, F. Cai, M. Ke, and Z. Liu, *Phys. Rev. E* **76**, 056605 (2007).
- ¹⁰B. M. Breid, D. Witthaut, and H. J. Korsch, *New J. Phys.* **8**, 110 (2006); **9**, 62 (2007); D. Witthaut, F. Trimborn, V. Kegel, and H. J. Korsch, *Phys. Rev. A* **83**, 013609 (2011).
- ¹¹S. Longhi, *Europhys. Lett.* **76**, 416 (2006); *Phys. Rev. Lett.* **101**, 193902 (2008).
- ¹²V. Krueckl and K. Richter, *Phys. Rev. B* **85**, 115433 (2012).
- ¹³F. Dreisow, A. Szameit, M. Heinrich, T. Pertsch, S. Nolte, A. Tünnermann, and S. Longhi, *Phys. Rev. Lett.* **102**, 076802 (2009).
- ¹⁴S. Kling, T. Salger, C. Grossert, and M. Weitz, *Phys. Rev. Lett.* **105**, 215301 (2010).
- ¹⁵D. Cai, A. R. Bishop, N. Grønbech-Jensen, and M. Salerno, *Phys. Rev. Lett.* **74**, 1186 (1995); F. Dominguez-Adame, V. A. Malyshev, F. A. B. F. de Moura, and M. L. Lyra, *ibid.* **91**, 197402 (2003); E. Diaz, F. Dominguez-Adame, Yu. A. Kosevich, and V. A. Malyshev, *Phys. Rev. B* **73**, 174210 (2006); F. A. B. F. de Moura, L. P. Viana, M. L. Lyra, V. A. Malyshev, and F. Dominguez-Adame, *Phys. Lett. A* **372**, 6694 (2008); T. Schulte, S. Drenkelforth, G. K. Büning, W. Ertmer, J. Arlt, M. Lewenstein, and L. Santos, *ibid.* **77**, 023610 (2008); S. Walter, D. Schneble, and A. C. Durst, *ibid.* **81**, 033623 (2010); S. Longhi, *Phys. Rev. B* **81**, 195118 (2010); C. Gaul, E. Diaz, R. P. A. Lima, F. Dominguez-Adame, and C. A. Müller, *Phys. Rev. A* **84**, 053627 (2011).
- ¹⁶M. Gustavsson, E. Haller, M. J. Mark, J. G. Danzl, G. Rojas-Kopeinig, and H.-C. Nägerl, *Phys. Rev. Lett.* **100**, 080404 (2008); D. O. Krimer, R. Khomeriki, and S. Flach, *Phys. Rev. E* **80**, 036201 (2009); C. Gaul, R. P. A. Lima, E. Diaz, C. A. Müller, and F. Dominguez-Adame, *Phys. Rev. Lett.* **102**, 255303 (2009).
- ¹⁷A. Buchleitner and A. R. Kolovsky, *Phys. Rev. Lett.* **91**, 253002 (2003); A. R. Kolovsky, *Phys. Rev. A* **70**, 015604 (2004).
- ¹⁸J. K. Freericks, *Phys. Rev. B* **77**, 075109 (2008); M. Eckstein and P. Werner, *Phys. Rev. Lett.* **107**, 186406 (2011).
- ¹⁹F. Claro, J. F. Weisz, and S. Curilef, *Phys. Rev. B* **67**, 193101 (2003); D. Souza and F. Claro, *ibid.* **82**, 205437 (2010).
- ²⁰W. S. Dias, E. M. Nascimento, M. L. Lyra, and F. A. B. F. de Moura, *Phys. Rev. B* **76**, 155124 (2007); W. S. Dias, M. L. Lyra, and F. A. B. F. de Moura, *Phys. Lett. A* **374**, 4554 (2010).
- ²¹R. Khomeriki, D. O. Krimer, M. Haque, and S. Flach, *Phys. Rev. A* **81**, 065601 (2010).
- ²²K. Kudo, T. Boness, and T. S. Monteiro, *Phys. Rev. A* **80**, 063409 (2009); K. Kudo and T. S. Monteiro, *ibid.* **83**, 053627 (2011).
- ²³S. Longhi and G. Della Valle, *Phys. Rev. B* **85**, 165144 (2012).
- ²⁴K. Winkler, G. Thalhammer, F. Lang, R. Grimm, J. H. Denschlag, A. J. Daley, A. Kantian, H. P. Büchler, and P. Zoller, *Nature (London)* **441**, 853 (2006).
- ²⁵S. Fölling, S. Trotzky, P. Cheinet, M. Feld, R. Saers, A. Widera, T. Müller, and I. Bloch, *Nature (London)* **448**, 1029 (2007).
- ²⁶See, for instance: G. Beni and P. Pincus, *Phys. Rev. B* **9**, 2963 (1974); J.-P. Gallinar, *ibid.* **11**, 4421 (1975); J. E. Hirsch, *Phys. Rev. Lett.* **53**, 2327 (1984); J. W. Cannon and E. Fradkin, *Phys. Rev. B* **41**, 9435 (1990); J. Callaway, D. P. Chen, D. G. Kanhere, and Q. Li, *ibid.* **42**, 465 (1990); P. G. J. van Dongen, *ibid.* **49**, 7904 (1994); A. P. Kampf and A. A. Katanin, *ibid.* **67**, 125104 (2003); Y. Z. Zhang, *Phys. Rev. Lett.* **92**, 246404 (2004); S.-J. Gu, S.-S. Deng, Y.-Q. Li, and H.-Q. Lin, *ibid.* **93**, 086402 (2004); Ka-Ming Tam, Shan-Wen Tsai, and David K. Campbell, *ibid.* **96**, 036408 (2006); A. Amaricci, A. Camjayi, K. Haule, G. Kotliar, D. Tanaskovic, and V. Dobrosavljevic, *Phys. Rev. B* **82**, 155102 (2010); F. Hofmann and M. Potthoff, *ibid.* **85**, 205127 (2012).
- ²⁷G. Pupillo, A. Griessner, A. Micheli, M. Ortner, D.-W. Wang, and P. Zoller, *Phys. Rev. Lett.* **100**, 050402 (2008); M. Ortner,

A. Micheli, G. Pupillo, and P. Zoller, *New J. Phys.* **11**, 055045 (2009).

²⁸This can be formally proven by an asymptotic analysis of Eq. (3) assuming the scaling $J/U \sim \epsilon$, $V/U \sim 1$, and $F/U \sim \epsilon$, where ϵ is a small parameter (see, for instance, Ref. 23).

²⁹J.-P. Nguenang and S. Flach, *Phys. Rev. A* **80**, 015601 (2009); J.-Pierre Nguenang, S. Flach, and R. Khomeriki, *Phys. Lett. A* **376**, 472 (2012).

³⁰S. Longhi, *Opt. Lett.* **36**, 3248 (2011); S. Longhi and G. Della Valle, *ibid.* **36**, 4743 (2011).